# Lawrence Berkeley Laboratory
UNIVERSITY OF CALIFORNIA

## ENERGY & ENVIRONMENT DIVISION

Published in Journal of Physics E: Scientific Instruments, Vol. 13, 1980, pp. 315-322

ASSOCIATING PARTICLE TRACKING WITH LASER FRINGE ANEMOMETRY

R.K. Cheng, M.M. Popovich, F. Robben, and F.J. Weinberg



September 1979



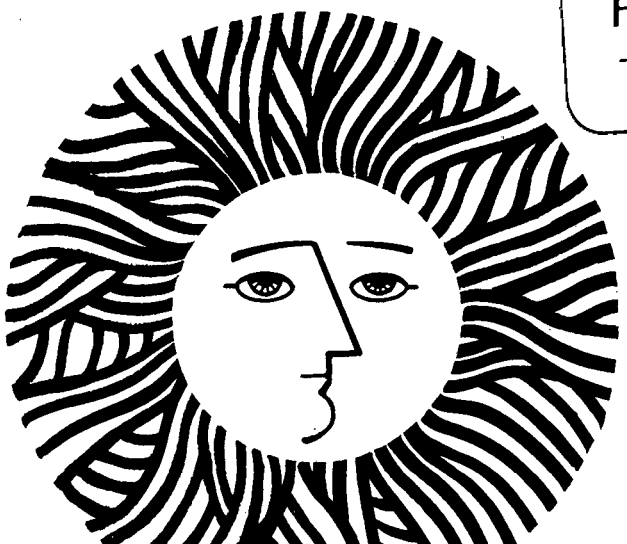

Prepared for the U.S. Department of Energy under Contract W-7405-ENG-48

## DISCLAIMER

## DISCLAIMER

J. Phys. E: Sci. Instrum., Vol. 13, 1980. Printed in Great Britain

# Associating particle tracking with laser fringe anemometry

**R K Cheng,† M M Popovich,‡ F Robben† and F J Weinberg‡**
† Lawrence Berkeley Laboratory, University of California, Berkeley, California, USA
‡ Imperial College, London SW7, UK

*Received 14 May 1979, in final form 20 September 1979*

**Abstract** In order to obviate the complementary limitations of velocimetry by laser fringe anemometry and by photographic particle tracking, a family of optical systems is described which is suitable for both types of measurement over extended test regions. It is based on a thin sheet of light from a powerful CW laser which is broken into fine interference fringes in its plane and interrupted at a known frequency. Depending on the divergence and energy density of the beam, various applications are considered ranging from test areas as large as those required in fire research to those more characteristic of high velocity applications which involve test space dimensions of several centimetres. The conflicting criteria of visibility of tracer particles and their ability to follow variations in gas flow are examined for these regimes. Among other capabilities of such systems are the addition of a third dimension by using multiple sheets of light, and the use of the fringes as visible 'ray trajectories' in deflection tracing through refractive index gradients.

## Introduction

The recording of velocity vectors at short exposure times by photographing the tracks of particles suspended in a flowing transparent medium and intermittently illuminated from the side by an intense light beam has been used extensively in combustion research (e.g. Andersen and Fein 1950, Fristrom *et al* 1953, Levy and Weinberg 1959, Tewari and Weinberg 1967, Fox and Weinberg 1962, Fristrom and Westenberg 1965). For slow flows, illumination by high-pressure AC gas discharges has often been employed (Levy and Weinberg 1959, Tewari Weinberg 1967), the frequency of interruption due to the waveform of the electrical supply providing convenient timing marks. At faster flows, flashbulbs have been used with a fast mechanical chopper to interrupt the light beam. It is a measure of how much illumination photographic flashbulbs provide that in the classical work of Andersen and Fein adequate results were obtained without any focusing or light condensing system. A much higher light flux is, of course, obtainable by using a condenser and this has been used in all recent work, notwithstanding the resulting diminution in the area of test space available for measurement. With the advent of powerful CW lasers, this restriction should no longer apply and unfocused beams have been used, e.g. for shadow interferometry, in fire research and other situations where large test areas are required (Creeden *et al* 1972).

In recent years, particle tracking and its derivatives (including the novel application of speckle photography, e.g. May 1979, Lohmann and Weigelt 1977) have been overshadowed by laser Doppler velocimetry (e.g. Durst *et al* 1976). It has been shown (Schwar and Weinberg 1969) that the beat frequency between two differentially Doppler shifted beams can always be regarded in terms of an interference fringe system moving across a point detector or a tracer particle traversing a stationary fringe system. The latter corresponds to the most frequently used arrangement, generally known as 'fringe anemometry' in which velocities are recorded in the focal volume of two interfering laser beams, generally as a function of time.

Photographic particle tracking and laser Doppler velocimetry suffer from complementary shortcomings. The latter requires a very long time to map out a velocity field, one point at a time. Quite slow variations, or fluctuations, in flow parameters during this time make it all but impossible to obtain distributions at all. To take an example from our field – combustion – it is not generally possible to make flame phenomena absolutely stationary so that the focal point of a fringe anemometer will move, with time, through different parts of the flame's structure. An instantaneous snapshot of velocity vectors freezes such movement (without omitting any essential information, as the phenomenon is merely drifting along or fluctuating slowly in a quasi steady state). Another shortcoming of LDV in turbulent systems is that, when beams traverse one or more turbulent phase boundaries, the signals recorded will not yield information confined to the focal point alone (Hong *et al* 1977).

The limitations of particle tracking in combustion studies have been widely analysed and discussed (see e.g. Fristrom and Westenberg 1965, Gaydon and Wolfhard 1979) The measuring volume is defined by the light-condensing system and can be narrowly confined. Optical effects of turbulence and refractive index gradients (Weinberg 1961) are minimised by focusing the test volume on the photographic emulsion using a wide aperture lens system, which is also required in order to collect as much light as possible. Those limitations which the method shares with LDV are further discussed below. An important difference of photographic particle tracking is that it cannot convey sequential information without the use of very high speed cine photography. Also, it has customarily been used with very much larger tracer particles. This, however, along with other characteristics of the two methods, is largely dependent on the types of light sources and tracer densities customarily used by the two schools of research. Clearly, very fine particles are photographable over appreciable areas at levels of illumination available from powerful CW lasers. Equally, fringe anemometry need not be confined to a tiny focal volume so long as the cloud of tracer particles is tenuous enough not to give rise to too many interfering signals. Even for a dense cloud, an extended fringe system can be used, with different regions being focused in turn on to a small photodetector area.

Accordingly we set out with the premise that both types of information are needed: time variant velocities at a point and distributions of velocity in space at one time (or a sequence of times). The complementarity of the information is equivalent to that between the Lagrangian and Eulerian systems of coordinates. Thus the optical system detailed below is based on a thin sheet of light from a 4 W argon-ion laser broken into fine interference fringes in its plane and interrupted at a

0022-3735/80/030315+08 $01.50 

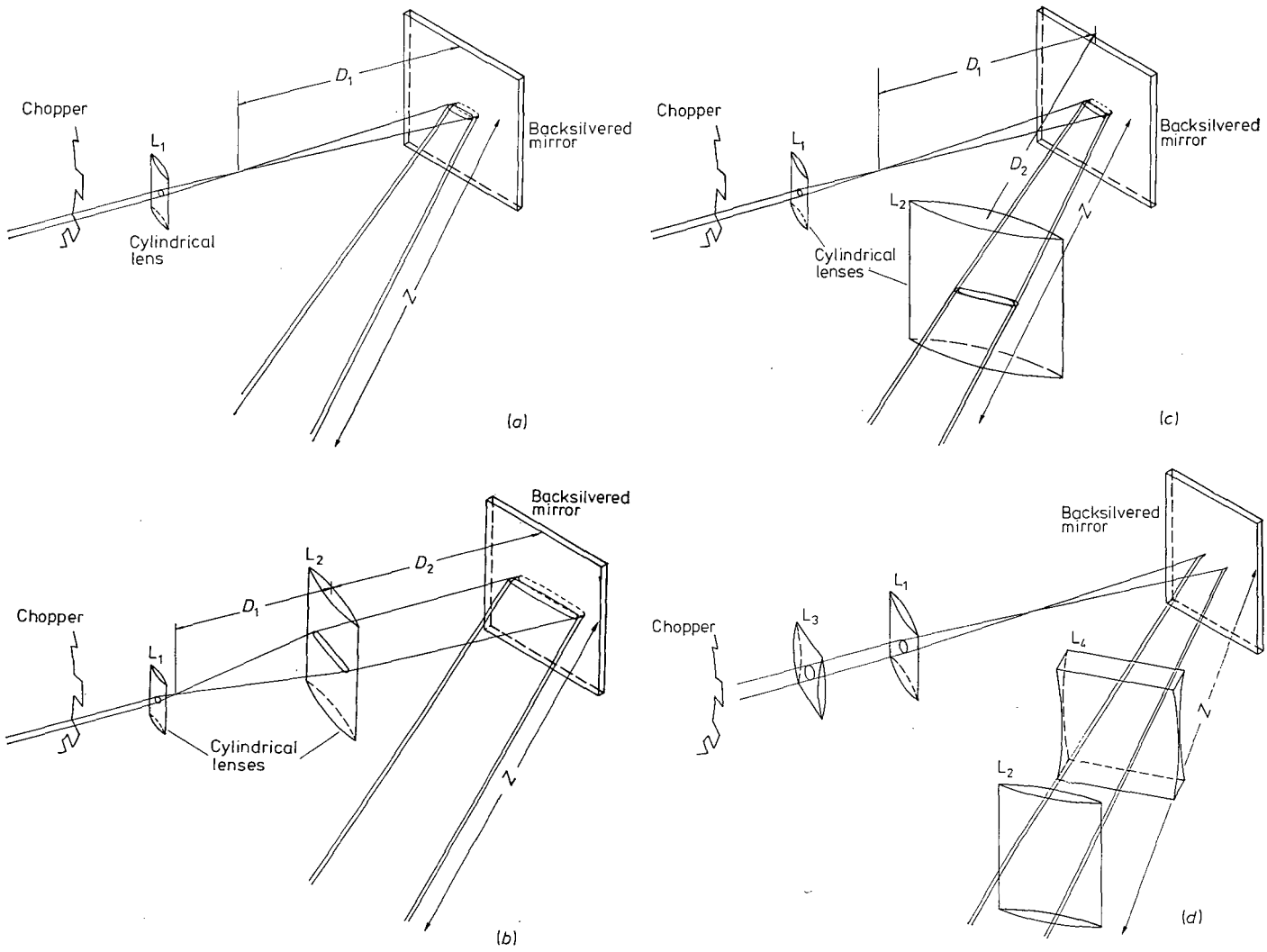


**Figure 1** Diagrams of optical systems.

known frequency, in order to fulfil both functions. This arrangement has several other interesting attributes.

## 2 Optical systems

A great many different optical systems, suitable for a variety of applications (some of which are illustrated in a later section) can be set up. Figure 1(*a*) illustrates the common principle. The laser beam, after being focused by a cylindrical lens, is simply sheared using the front and rear surface reflections from a thin glass slab (such as a microscope slide) at oblique incidence. This results in two wave fronts at a small angle to one another emanating from the two images of the focus. It follows from elementary optics that interference between the two diverging wavefronts gives rise to a fringe spacing

$$q=\frac{\lambda\eta(\eta_g{}^2-\cos^2\gamma)}{e\sin 2\gamma} \tag{1}$$

where $\eta$ is the distance between the plane of the record and the images of the focus, $\lambda$ the wavelength, $e$ and $n_g$ the thickness and refractive index of the glass slab, respectively, and $\gamma$ is the angle at which the incident beam impinges on it. A similarly simple device based on spherical lenses has been used before (Creeden *et al* 1972) for infinitesimal shear interferometry over large areas. In the present instance however, cylindrical lenses are used to produce a thin sheet of light, the fringes lie in its plane and in the direction of the optical axis. Thus in figure 1(*a*) the light sheet is allowed to retain the initial width of the laser beam, unmodified by any curved optical elements. In the notation of figure 1(*a*)

$$\eta=D_1+Z \tag{2}$$

and hence

$$q=\frac{\lambda}{e}(D_1+Z)\frac{(n_g{}^2-\cos^2\gamma)}{\sin 2\gamma} \tag{3}$$

where $Z$ is the distance between the last optical element and the plane of the record.

The additional facility offered by the second cylindrical lens $L_2$ introduced in figures 1(*b*) and (*c*) is that the divergence of the beam is no longer solely dependent on the focal length of the first lens. Figure 1(*b*) allows for the possibility of a non-divergent–i.e. near parallel–beam. Fringes, of course, disappear for parallelism of the emerging beam in the arrangement in figure 1(*c*) which, however, has the advantage that the angle of incidence to the beam splitter, and hence the fringe spacing, can be altered without re-aligning the second lens. The distance $\eta$ in the two cases is

$$\eta=Z+D^* \tag{4}$$

where

$$D^* = \frac{f_2(D_1 + D_2)}{f_2 - D_1 - D_2} \tag{5}$$

in the notation of figure 1b, $f_2$ being the focal length of $L_2$, and

$$D^* = \frac{f_2 D_1}{f_2 - D_1} + D_2 \tag{6}$$

in the notation of figure 1(*c*). The fringe spacing in the two cases is therefore

$$q = \frac{\lambda}{e}(Z + D^*)\frac{(n_g^2 - \cos^2\gamma)}{\sin 2\gamma}. \tag{7}$$

The divergence determines the width of the test space illuminated and hence also the light flux incident upon the tracer particles. Large divergences are necessary for test objects of the size encountered in fire research. Because of the need to study turbulence of extremely large scales, small models would not be representative and the dimensions of the test objects required preclude the use of any optical elements in the expanded beam. Fortunately, the velocity gradients' encountered under these circumstances are relatively small, allowing the use of larger tracer particles and hence lower light fluxes (see below). High-speed flow applications, on the other hand, tend to involve much smaller test areas and the greater light flux permits the use of smaller tracers.

It is not necessary to base the width of the light sheet, on whatever flux distribution emerges from the laser. Figure 1(*d*) illustrates a system in which this width can be varied by the use of two additional lenses $L_3$ and $L_4$, thereby providing another means of controlling the light flux in the test space. The fringe spacing is the same as in figure 1(*b*).

If the beam is also sheared by a beam splitter at right angles to the diagram in figure 1, the resulting 'fringe' pattern is equivalent to producing multiple light sheets. By keeping these few in number (wide 'fringe spacing') the system can be used for three-dimensional visualisation (see below).

In the photographic mode, the exposure time does not play the usual role of regulating the density of light reaching the film from each particle. The brightness of the track is a function of particle size, velocity, light flux in the test space and camera magnification. The exposure time determines the total length of the track and the total number of tracks on the record. Varying the exposure time is in some way analogous to varying the particle cloud density and very long exposure times will produce effects similar to the use of smoke as a tracer.

This has an interesting application to ray tracing. The interference fringes on the light sheet are everywhere perpendicular to the wave fronts (which are at a minute angle to one another) and therefore represent the local 'ray directions'. Ray tracing or 'deflection mapping' has been used extensively (e.g. Levy and Weinberg 1959, Weinberg 1961) for the quantitative analysis of refractive index fields in combustion research. It is possible to show up such ray trajectories and map refractive index fields either by using smoke or, in the case of steady state phenomena, by employing exceedingly long exposure times using normal particle seeding in the velocity measuring systems described.

In the photographic mode used for velocity tracking, the measurement of the time intervals is, of course, based on the chopper frequency, the interruptions due to interference fringes, arranged to be much finer, merely acting as a yardstick for measuring the length of the time-modulated tracks. The provision of such a length scale on every part of the record is extremely convenient because it makes the method independent of any distortion of the photographic emulsion during processing. Different chopper frequencies have been used for different ranges of velocities but, in general, the aim has been to create as long an illuminated period as possible. This not only improves accuracy but allows one to distinguish at once particles which have a large velocity component at right angles to the sheet by their short tracks due to their brief periods of residence within it. Similarly it is preferable to use chopper configurations which allow longer 'on' than 'off' times, producing longer tracks for a given number of interruptions (an on/off ratio of 70/30 was used in much of this work). Particles with small velocity components perpendicular to the light sheet are identifiable by their shorter total illuminated trajectories as well as by their smaller velocity component in the plane studied.

In the fringe anemometry mode, the chopper is not required, though it will provide independent timing marks when scattered from a stationary test object (just as the fringes provide an independent measuring stick for the time-modulated photographic mode). The main difference from conventional LDV systems is that the whole light sheet is potentially available as the scattering volume, the total area being limited only by the light power density available. Using imaging optics analogous to that of the camera in the photographic mode to focus the test space on a photo-detector of appreciable area, an aperture in a mask placed in the image plane can be used to select any particular part of that volume (instead of mounting the entire input and collecting optics on movable carriers which travel together). The size of the aperture is determined by the spatial resolution required which, in turn, depends on flow parameters such as the scale of turbulence. The density of the cloud of tracer particles must be chosen in conjunction with aperture size to control the frequency of signal occurrence. The main advantage of the system is simplicity, lower cost and, because of the much lower inertia of the moving parts, that more rapid traverses can be carried out by moving the aperture rather than the entire optical system or test object – which would be necessary with most conventional methods. In the case of test objects as large as those used in fire research, for example, conventional optical systems could not be used without immersing them in the hot gases or redesigning them to work with such long focal lengths that the test volume would become very large. With several photo-detectors it is possible also to measure velocity fluctuations in several regions simultaneously using a single optical system. Even with two, signal correlations at two points of variable separation are rapidly obtainable with the same fringe system. It is also worth noting that the present system is much simpler than most other fringe anemometers and requires no expensive optical components, once a laser of sufficient power is available.

## 3 Selection of suitable tracers

The major criteria in choosing tracer particles are that they should be able to follow fluctuations of the flow without a significant lag in velocity and that they scatter enough light for easy recording. The two requirements, of course, conflict. The former calls for small light particles. As regards the latter, the light received at the detector, for a given geometry of the optical system, is a sensitive function of particle size, shape, and refractive index (e.g. Kerker 1962). The dependence on particle radius is particularly strong, the larger particles within the range of interest scattering several orders of magnitude more light than the smallest.

The lag in velocity $\Delta v$ can be approximated by equation (8) where the Stokes law drag on a spherical particle of radius $r$

is balanced by the acceleration force:

$$ma = 6\pi r\mu\Delta v. \tag{8}$$

In equation (8), $m$ is the mass of the particle, $\mu$ is the viscosity of the fluid and $a$ the particle acceleration. Stoke's law is generally applicable on the assumption that the particle velocity is near enough to that of the gas to make their relative Reynolds number exceedingly small.

For the relatively high velocity applications discussed in the next section, aluminium oxide particles were used. The permissible maximum size was calculated on the basis of the following values for the relevant parameters: $a$ was taken to be $2\sqrt{\overline{u^2}w}$, where $\sqrt{\overline{u^2}}$ is the root-mean-square velocity of the fluctuations, while $w$ is its frequency. $\sqrt{\overline{u^2}}$ was assumed to be 10% of the mean velocity and $w$ was assumed to be 100 Hz. Our calculation indicated that $\Delta v/\sqrt{\overline{u^2}}$ will be less than 1·0% for particles smaller than 5 $\mu$m. This, together with the sensitivity of the photomultiplier or photographic emulsion and the magnification of the image of the test space defines the minimum light flux required. For a given laser and a light sheet of a particular width, this in turn defines the maximum size of test space which can be examined at one time. The general principles underlying such calculations have been summarised e.g. in Soo (1967), Boothroyd (1972) and Mazumder and Kirsch (1975).

A simple and convenient experimental method of correlating these parameters is to plot the maximum area of the light beam over which photographable tracks are obtainable against the free fall velocity $v_f$ of the particle. $v_f$ is of course directly measurable by applying the methods here described in the absence of any flow velocity. It is directly related to the relevant parameters in equation 8 by

$$(4/3)\,\pi r^3(\rho_p - \rho_g)\,g = 6\pi r\mu v_f \tag{9}$$

where $g$ is the acceleration due to gravity and $(\rho_p - \rho_g)$ represents the difference in density between the particle and the gas. The velocity lag of equation 8, $\Delta v$, can then simply be expressed as

$$\Delta v = \frac{a}{g} v_f \tag{10}$$

on the supposition that the gas density is negligible by comparison with that of the particle.

This approach has been employed in the case of the much larger areas – of the order of square metres – used in fire research where it becomes necessary to use much larger tracer particles so that sufficient scattered light can be collected for photographic purposes. Since the velocities in fires, being due to natural convection, tend to be smaller than those discussed in the paragraphs above, it is worthwhile to minimise $\rho_p$ so as to allow the use of larger particles. In the work inside turbulent plumes, ground polystyrene particles were used because of their low density and excellent light scattering properties. The only restrictions on their use occurs at high flame temperature however, in the zones of particular interest to the work on fire plumes, most of the gas is entrained and therefore not at a high temperature.

The above theory applies to spherical particles and cannot be readily generalised to particles of indeterminate, or mixed, shapes. These, however, tend to fall (or orientate themselves to any other relative gas velocity) in a preferred direction so as to minimise the drag force equivalent to the right hand side of equations (8) and (9). In order to base particle size on the relevant parameter, the polystyrene particles were graded by their free fall velocity, using an elutriator at various flow velocities. Such a sizing procedure automatically selects the appropriate parameter.

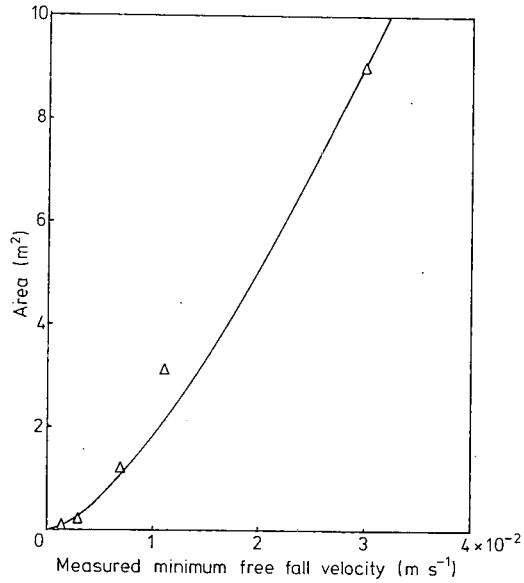


**Figure 2** Useful illuminated area plotted against measured minimum free fall velocity of tracers.

Figure 2 illustrates the behaviour of polystyrene particles in terms of the relationship between the maximum area of test space illuminated and the observed free fall velocity. This covers the opposite extreme to the micrometre size particles discussed above. It will be seen that for areas of the order of 1 m², free fall velocities of the order of several millimetres per second are recorded, while 3 cm s$^{-1}$ (which is still only 3% of a flow velocity of 1 m s$^{-1}$) extends test section areas up to 9 m²!

## 4 Applications

Examples of applications are drawn from opposite ends of the test space area range; these happen to correspond to the fields of interest of our two schools of research. The small test section work carried out at the Lawrence Berkeley Laboratory employed the optical system of figure 1(*b*) using cylindrical lenses of 3·3 and 40 mm focal length. The frequency of the mechanical chopper was monitored by an oscilloscope and the test section flow field was generated by a stagnation chamber of 20 cm diameter, with a 5 cm diameter nozzle.

Three groups of experiments are illustrated: velocity measurement in an air stream emerging from the nozzle, velocity distributions in the flow field of a V-shaped flame stabilised on a heated wire and visualisation of the wake generated by a cylindrical rod. The width of the slightly divergent beam was arranged to be about 3·0 cm at the test space with a separation between fringes of 0·33 mm. The range of flow velocities of interest was 10–10$^3$ cm s$^{-1}$ which was split into two ranges using different chopper plates and sizes of $Al_2O_3$ tracer particles. 2–5 $\mu$m particles were used up to about 500 cm s$^{-1}$ and 10–20 $\mu$m particles at higher velocities. This was based on light from a 4 W argon-ion laser which delivered approximately 1·2 W at 488 $\mu$m, particle tracks being recorded on Polaroid type 57 (ASA 3000) film using a camera objective of 116 mm focal length at $f$/4·5. It is worth noting that had the laser been operated at full power (all lines) the use of larger particles would have been unnecessary. Clearly there is also much further scope for increasing the track brightness by narrowing the width of the beam (see

figure 1(*c*)), increasing the numerical aperture of the lens or decreasing magnification, should this be required.

For fringe anemometry, a 55 mm focal length lens was used to image the scattered light onto a photomultiplier through a pinhole. The signal from the photomultiplier tube was displayed on an oscilloscope. The magnification was such that a 0·05 mm pinhole selected an area of about 1·7 mm diameter, containing five fringes.

On much larger scales, work is proceeding on the measurement of velocity distributions in turbulent fire plumes. The model fires are produced by burning methanol in circular pans of diameters ranging from 3–15 cm. Since the test areas studied are of the order of 1 $m^2$, the parallel fringe mode of the instrument is unsuitable. To obtain the necessary coverage of large areas, the laser beam is expanded into a divergent sheet, using the system of figure 1(*c*). The particle tracks were photographed, using a 16 mm cine camera, on Ilford FP 4 16 mm cinematographic film. Ground polystyrene tracers of minimum diameter in the range 600 to 800 $\mu$m were introduced into the test space from a fluidised bed elutriator. The cine camera framing rate could be varied from 1–8 frames $s^{-1}$ with individual frame exposure times in the range 1/25 to 1 s. The thickness of the sheet of light was typically of the order of a few millimetres, which is generally quite negligible by comparison with the width of the plume being studied.

For the slowest of the velocities, the exposure duration can

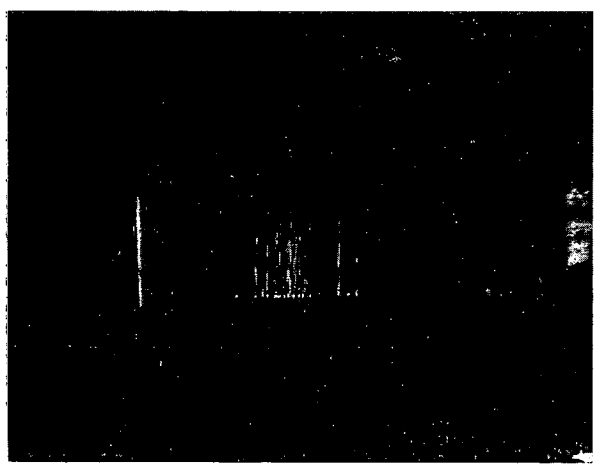

(*a*)

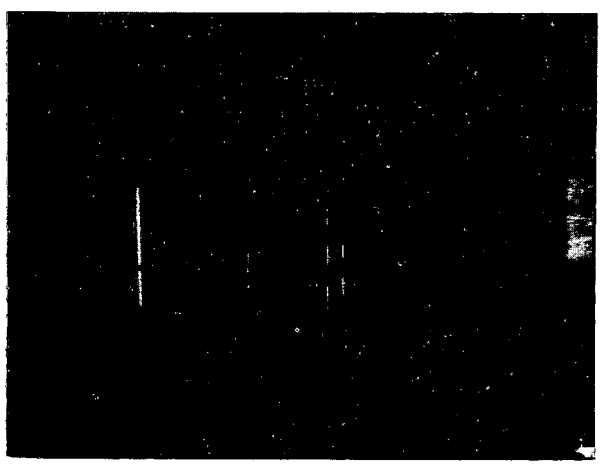

(*b*)

**Figure 3** Examples of particle tracking over small areas in air stream emerging from a nozzle; (*a*) 3·0 m $s^{-1}$, (*b*) 6·67 m $s^{-1}$.

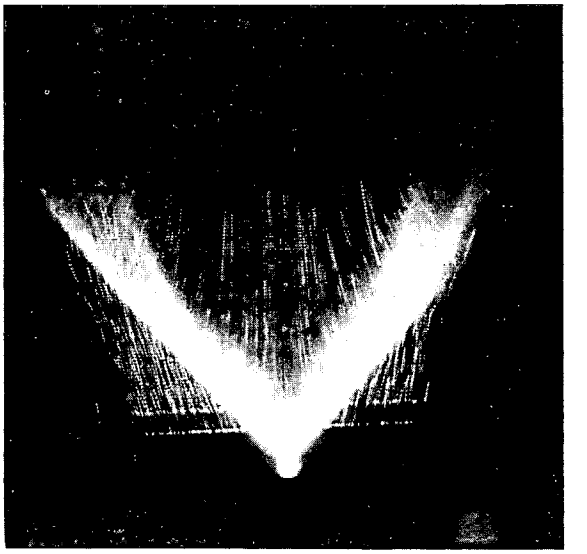

(*a*)

(*b*)

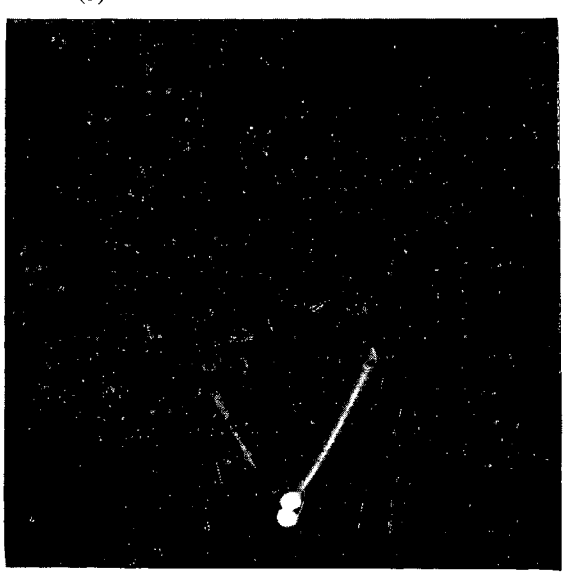

(*c*)

**Figure 4** Flow field of a V-shaped natural gas flame stabilised on a heated platinum wire at varying exposure times; (*a*) 1/2, (*b*) 1/10, (*c*) 1/25 s.

be used as the time standard instead of the period of illumination given by a chopper. This will result in a single long track per particle (except for the spatial modulation due to interference fringes) but, since the shutter motion is synchronised with that of the film, the cut off is quite sharp – see figure 5.

Examples of particle tracking over small areas in the air stream emerging from the nozzle are shown in figures 3(*a*) and (*b*). The fringes on the light sheet are clearly visible. Both records were taken with an exposure time of 1/2 s (*f*/4·5) and the particles seeded in the flow were of 2 $\mu$m size. The difference in the light track density is due to the difference in particle cloud density. Chopping frequencies were 100 Hz for figure 3(*a*) and 167 Hz for figure 3(*b*). These frequencies produce three to four interruptions on each track for this velocity range.

Figures 4(*a*), (*b*) and (*c*) show particle tracking in the flow field of a V-shaped natural gas flame stabilised on a heated platinum wire. Chopping frequency for all three records was 66·7 Hz, and the exposure times were 1/2, 1/10 and 1/25 s for figures 4(*a*), (*b*) and (*c*) respectively. The changes in flow direction as well as the acceleration across the flame front are quite apparent. The amplitude of the fluctuation of the flame front is indicated by the thickness of the luminous zone in figure 4(*a*). This illustrates the difficulty that would be encountered in attempting to measure velocity distribution by conventional LDV methods. As can be seen by comparison of the records, the thickness of this zone is reduced as exposure time is decreased until exposure time is sufficiently short (figure 4(*c*)) for the luminous zone to become thin enough to indicate the true flame thickness and orientation. Local burning velocity can then be measured by the component of the velocity vector perpendicular to the flame front.

As an illustration of the very slowest velocities, figure 5 shows a cine sequence of tracks of particles used in fire plumes at close to free fall velocity. The single illumination period on each frame is fixed by the exposure time of 1 s, as discussed above. The framing rate was 1 frame $s^{-1}$ and the velocity distribution in space and time is measured over an area of 1300 $cm^2$. The size of the polystyrene particles used was in the range 600–800 $\mu$m. Equivalent information at a point can be obtained without a cine camera by measurements in the fringe anemometry mode – a typical signal obtained in a fire plume, using fringe spacing as large as 1 cm is illustrated in figure 6. By contrast a snap-shot covers an appreciable area but, does not, of course, indicate the sequence of the events recorded. An illustration of varying exposure time is given in figures 7(*a*), (*b*) and (*c*) which show the wake generated by a rod of 4 mm diameter placed in gas flowing at 122 cm $s^{-1}$, at exposure times of 1, 1/2 and 1/5 s, respectively. The crossing of flow vectors at the longer exposures does not imply that the flow is not unidirectional at every point and every instant in time. It shows successive events due to the exposure time being appreciable on the scale of the period of eddy shedding.

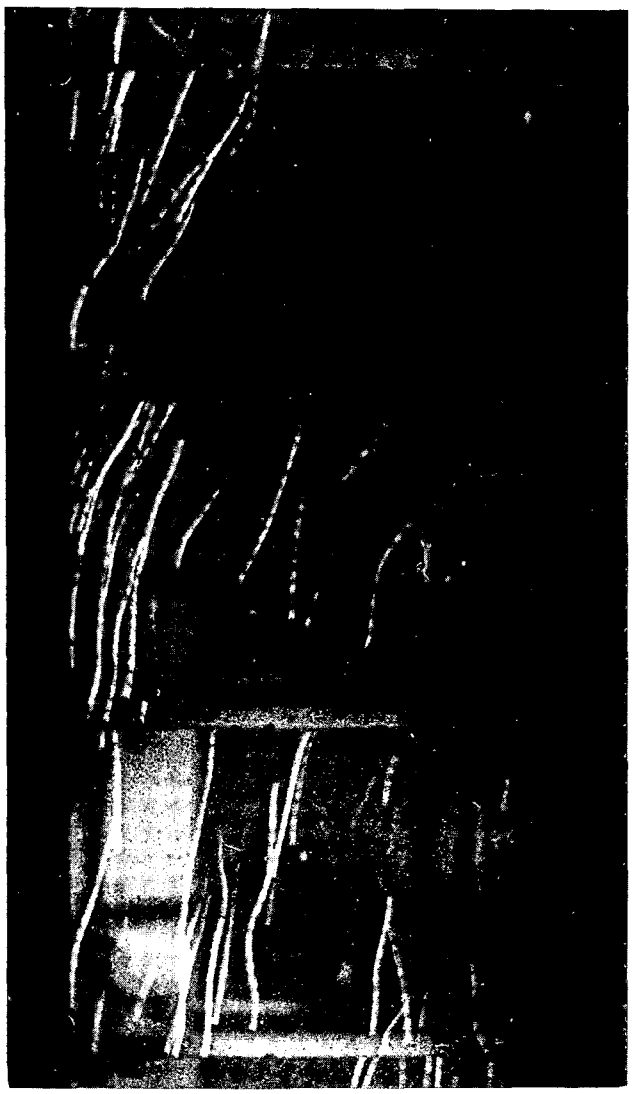

**Figure 5** Cine sequence of particle tracks in fire plume at close to free fall velocity of the tracers. Area covered is 1300 $cm^2$.

**Figure 6** Fringe anemometry oscillogram with wide (1 cm) fringe spacing.

Figures 8(*a*), (*b*) and (*c*) illustrate the ray tracing facility discussed earlier. These were not in fact produced by using long exposure times but by employing smoke as a tracer. Figure 8(*c*) illustrates the focusing of the beam shown in figure 8(*a*) by a lens and is a convenient way of showing up lens aberrations, while figure 8(*b*) shows the effect of a temperature gradient. In this, a heated aluminium rod was placed along the top edge of the beam. Under these conditions the 'ray trajectories' follow the relationship (see e.g. Weinberg 1961).

$$\frac{1}{R} = -\frac{1}{n}\frac{\partial n}{\partial R} \tag{6}$$

(*a*)

(*b*)

(*c*)

**Figure 7** Particle tracking in the wake of a rod at varying exposure times; (*a*) 1 s, (*b*) 1/2 s, (*c*) 1/5 s.

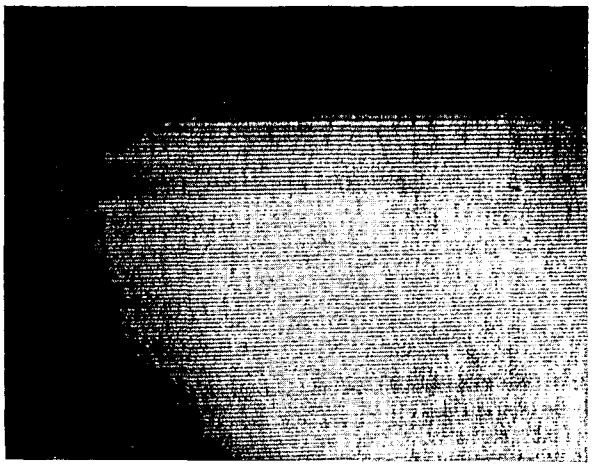

(*a*)

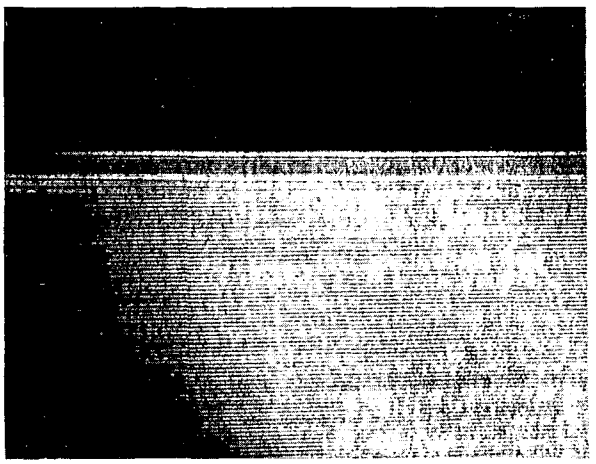

(*b*)

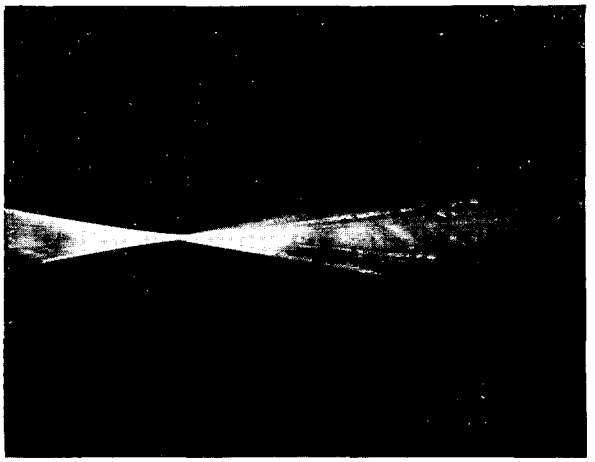

(*c*)

**Figure 8** Ray tracing by fringes; (*a*) unperturbed beam, (*b*) deflection due to temperature gradient, (*c*) near the focus of the lens.

where $R$ is the local radius of curvature of the ray and $n$ is the refractive index. The photograph shows the results of refraction and overlap of the beams.

Finally, figure 9 shows a vortex propagating in air after ejection from an aperture, sectioned by eight light sheets, using visualisation by smoke. The exposure time was 1/25 s and the vortex diameter approximately 13 cm.

Although this method does not offer the continuity in the third dimension of a hologram, it does give a three-dimensional representation on a two-dimensional photograph and, unlike a hologram, does not require reconstruction.

The purpose of the particular measurements used as examples above will be published elsewhere. The object of this note is to draw attention to the versatility and power of this simple and inexpensive optical tool.

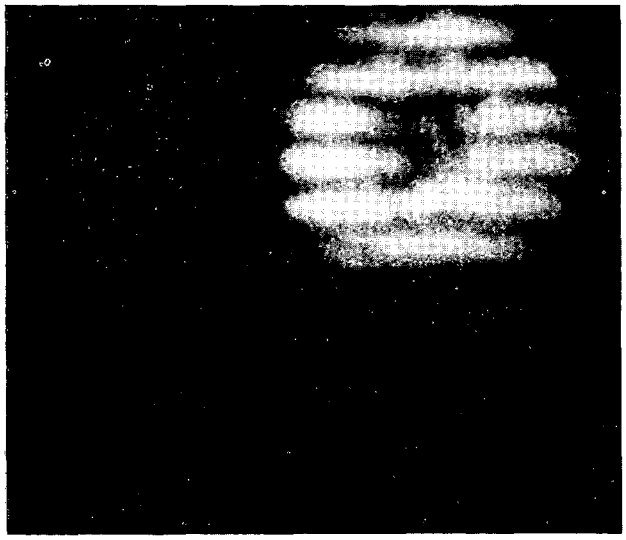

**Figure 9** 'Smoke Ring' vortex sectioned by multiple light sheets.

**Acknowledgments**

We are indebted to the Joint Fire Research Station of the UK Department of the Environment for financial support including a bursary to one of us (MMP), and to the Basic Energy Science Division of the US Department of Energy under contract No W-7405-ENG-48.

**References**

Andersen J W and Fein R S 1950 Measurement of normal burning velocities of propane air flames from shadow photographs
*J. Chem. Phys.* **18** 441

Boothroyd R G 1972 Tracer behaviour in laser anemometry for turbulent flow
*Opt. Laser Technol.* **4** 2

Creeden J E, Fristrom R M, Grunfelder C and Weinberg F J 1972 A large-area differential laser interferometer for fire research
*J. Phys. D: Appl. Phys.* **5** 1063

Durst F, Melling A and Whitelaw J H 1976 *Principles and Practice of Laser Doppler Anemometry* (London: Academic)

Fox M D and Weinberg F J 1962 An experimental study of burner stability of turbulent flames in premixed reactants
*Proc. R. Soc. A* **268** 222

Fristrom R M, Prescott R, Neumann R K and Avery W H 1953 Temperature profiles in propane-air flame fronts.
*4th Symp. (International) on Combustion* (Baltimore: Williams & Wilkins) p 267

Fristrom R M and Westenberg A A 1965 *Flame Structure* (New York: McGraw-Hill)

Gaydon A G and Wolfhard H G 1979 *Flames* (London: Chapman & Hall)

Hong N S, Jones A R and Weinberg F J 1977 Doppler velocimetry within turbulent phase boundaries
*Proc. R. Soc.* A **353** 77

Kerker M 1963 *Electromagnetic Scattering, Proc. Inter-disciplinary Conference, Potsdam, New York*, August 1962 (New York: Pergamon)

Levy A and Weinberg F J 1959 Optical flame structure studies: examination of reaction rate laws in lean ethylene air flames
*Combustion and Flame* **3** 229

Lohmann A W and Weigelt G P 1975 The measurement of motion trajectories by speckle photography
*Opt. Commun.* **14** 252

May M 1979 Information derived from speckle patterns
*J. Phys. E: Sci. Instrum.* **10** 849

Mazumder M K and Kirsch K J 1975 Flow tracing fidelity of scattering aerosol in laser Doppler velocimetry
*Appl. Opt.* **14** 894

Schwar M J R and Weinberg F J 1969 The measurement of velocity by applying Schlieren interferometry to Doppler shifted laser light
*Proc. R. Soc.* A **311** 469

Soo S L 1967 *Fluid Dynamics of Multiphase Systems* (Boston: Ginn)

Tewari G P and Weinberg F J 1967 Structure of flame quenched by cold surfaces
*Proc. R. Soc.* A **296** 546

Weinberg F J 1961 *Optics of Flames* (London: Butterworths)

*TECHNICAL INFORMATION DEPARTMENT*
*LAWRENCE BERKELEY LABORATORY*
*UNIVERSITY OF CALIFORNIA*
*BERKELEY, CALIFORNIA 94720*